PLOS ONE

RESEARCH ARTICLE

Concatemeric Broccoli reduces mRNA stability and induces aggregates

Marco R. Rink[1,2], Marisa A. P. Baptista[1], Felix J. Flomm[3,4,5,6], Thomas Hennig[1], Adam W. Whisnant[1], Natalia Wolf[7], Jürgen Seibel[7], Lars Dölken[1,8], Jens B. Bosse[3,4,5,6]*

1 Institute for Virology and Immunobiology, Julius-Maximilians-University Würzburg, Würzburg, Germany, **2** Centre for Liver and Gastrointestinal Research, Institute of Immunology and Immunotherapy University of Birmingham, Birmingham, United Kingdom, **3** Centre for Structural Systems Biology, Hamburg, Germany, **4** Cluster of Excellence RESIST (EXC 2155), Hannover Medical School, Hannover Medical School, Hannover, Germany, **5** Leibniz Institute for Experimental Virology (HPI), Hamburg, Germany, **6** Hannover Medical School, Institute of Virology, Hannover, Germany, **7** Institute of Organic Chemistry, Julius-Maximilians-University Würzburg, Würzburg, Germany, **8** Helmholtz Institute for RNA-based Infection Research (HIRI), Helmholtz-Center for Infection Research (HZI), Würzburg, Germany

* jens.bosse@cssb-hamburg.de

Citation: Rink MR, Baptista MAP, Flomm FJ, Hennig T, Whisnant AW, Wolf N, et al. (2021) Concatemeric Broccoli reduces mRNA stability and induces aggregates. PLoS ONE 16(8): e0244166. https://doi.org/10.1371/journal.pone.0244166

Editor: Ian B. Hogue, Arizona State University, UNITED STATES

Received: December 2, 2020

Accepted: July 17, 2021

Published: August 4, 2021

Data Availability Statement: All relevant data are within the paper and its Supporting Information files.

Funding: LD: Infect-ERA grant eDEVILLI JB: DFG (German Research Foundation, www.dfg.de) EXC 2155 "RESIST" – Project ID 390874280 AWW: Humboldt Foundation and the German Federal Foreign Office FJF: graduate student fellowship by the Studienstiftung des deutschen Volkes The funders had no role in study design, data collection and analysis, decision to publish, or preparation of the manuscript.

Abstract

Fluorogenic aptamers are an alternative to established methodology for real-time imaging of RNA transport and dynamics. We developed Broccoli-aptamer concatemers ranging from 4 to 128 substrate-binding site repeats and characterized their behavior fused to an mCherry-coding mRNA in transient transfection, stable expression, and in recombinant cytomegalovirus infection. Concatemerization of substrate-binding sites increased Broccoli fluorescence up to a concatemer length of 16 copies, upon which fluorescence did not increase and mCherry signals declined. This was due to the combined effects of RNA aptamer aggregation and reduced RNA stability. Unfortunately, both cellular and cytomegalovirus genomes were unable to maintain and express high Broccoli concatemer copy numbers, possibly due to recombination events. Interestingly, negative effects of Broccoli concatemers could be partially rescued by introducing linker sequences in between Broccoli repeats warranting further studies. Finally, we show that even though substrate-bound Broccoli is easily photobleached, it can still be utilized in live-cell imaging by adapting a time-lapse imaging protocol.

Introduction

RNA aptamers are short RNA sequences that exert specific binding abilities to a given biological structure or small molecule. Fluorogenic RNA aptamers in this regard are characterized by their ability to bind a small molecule and greatly enhance its fluorescence potential. This has been first reported with an aptamer called Spinach [1] (the name due to its green fluorescence) and been further expanded over the recent years with other aptamers emerging, such as the RNA Mangos [2], Broccoli [3] or Corn [4]. The most prevalent RNA aptamers are RNA mimics of GFP, termed as such by the very similar peak excitation and emission wavelengths. Mechanistically these aptamers consist of binding a GFP mimicking small molecule

Competing interests: The authors have declared that no competing interests exist.

fluorophore, thereby inhibiting vibration and isomerization, forcing fluorescence as the only remaining mechanism to dissipate energy [5]. As such, the aptamer itself becomes visible when its substrate is present, the substrate in its unbound state is non- or only lowly fluorescent. For this, the most widely used substrate is DFHBI ((5Z)-5-[(3,5-Difluoro-4-hydroxyphenyl)methylene]-3,5-dihydro-2,3-dimethyl- 4H-Imidazol-4-one) or a derivative thereof, which are generally membrane permeable.

Due to these features, RNA aptamers, when fused to an RNA of interest, can be utilized to detect RNAs in living cells by all common methodologies that utilize fluorescence, e.g. flow cytometry or fluorescence microscopy and constitute an alternative to the "gold-standard" for RNA imaging, the MS2-tagging system [6]. Tandem arrays of MS2-tags fused to a given RNA have tremendous RNA tracking potential potentially providing single-molecule resolution [7]. An optimal RNA tag would enable researchers to visualize single RNA molecules without perturbing their normal biological properties and behavior. Here, RNA aptamers were proposed to potentially have a smaller impact on the biological properties of the tagged RNA molecule.

Fluorescent RNA aptamers have now been used to elucidate many fundamental RNA biology processes, including transcription rates [4] and RNA aggregate studies [8]. Especially when high concentrations of RNA are present within a structure, the aptamer approach should provide insights into cell's RNA biology. As such, p-bodies, stress granules, rRNAs and small non-coding RNAs and their dynamics are especially interesting. Single aptamer tags so far have not been successful in the tracking or quantification of single molecules though, but reminiscent of the MS2-tag concatemers, tandem arrays could greatly empower the scope of the methodology. Recently, the tandem array approach has been successfully utilized, in bacteria [9], and, with a new substrate, to visualize overexpressed RFP carrying mRNA molecules in mammalian cells [10]. However, the introduction of multiple extensively structured exogenous sequences into a given RNA molecule may alter the physiological behavior of the respective molecules. This question has been addressed by Li *et al*. and they determined no effect of the repeated Broccoli RNA aptamer on mRNA stability [10]; quite different to our experience with it.

Here, we report on the development of high copy number Broccoli RNA aptamer tandem arrays and their effects on RNA export, localization and stability, with the scope of using the system to visualize and track viral RNAs in productive virus infection.

Results

In order to perform high-resolution microscopy for single-molecule imaging in mammalian cells, we generated tandem arrays of the aptamer Broccoli. We expanded the number of binding sites for the fluorochrome DFHBI from 4 to 128 copies by repetitive duplications (strategy described in the methods section and in Fig 1A; refer to S1 and S2 Tables for nomenclature and insert sequence length). The coding sequence (CDS) of the fluorescent protein mCherry was inserted upstream of the Broccoli tandem arrays to monitor their effects on protein expression.

To determine the fluorescence intensity of each Broccoli tandem array, 293T cells were transfected with the Broccoli-expressing plasmids and 24 hours later the cells were collected, resuspended in PBS buffer containing DFHBI, and analyzed by flow cytometry (Fig 1B). While 4x Broccoli only resulted in a weak green fluorescence in mCherry positive cells, green fluorescence doubled from 4x to 8x Broccoli. Although a small further increase in green signal was observed for 16x Broccoli, no further increase was observed thereafter (Fig 1C). While 44% of the cells were mCherry-positive when transfected with an mCherry-only control plasmid, the percentage of mCherry-positive cells decreased with increasing size of the Broccoli reporter.

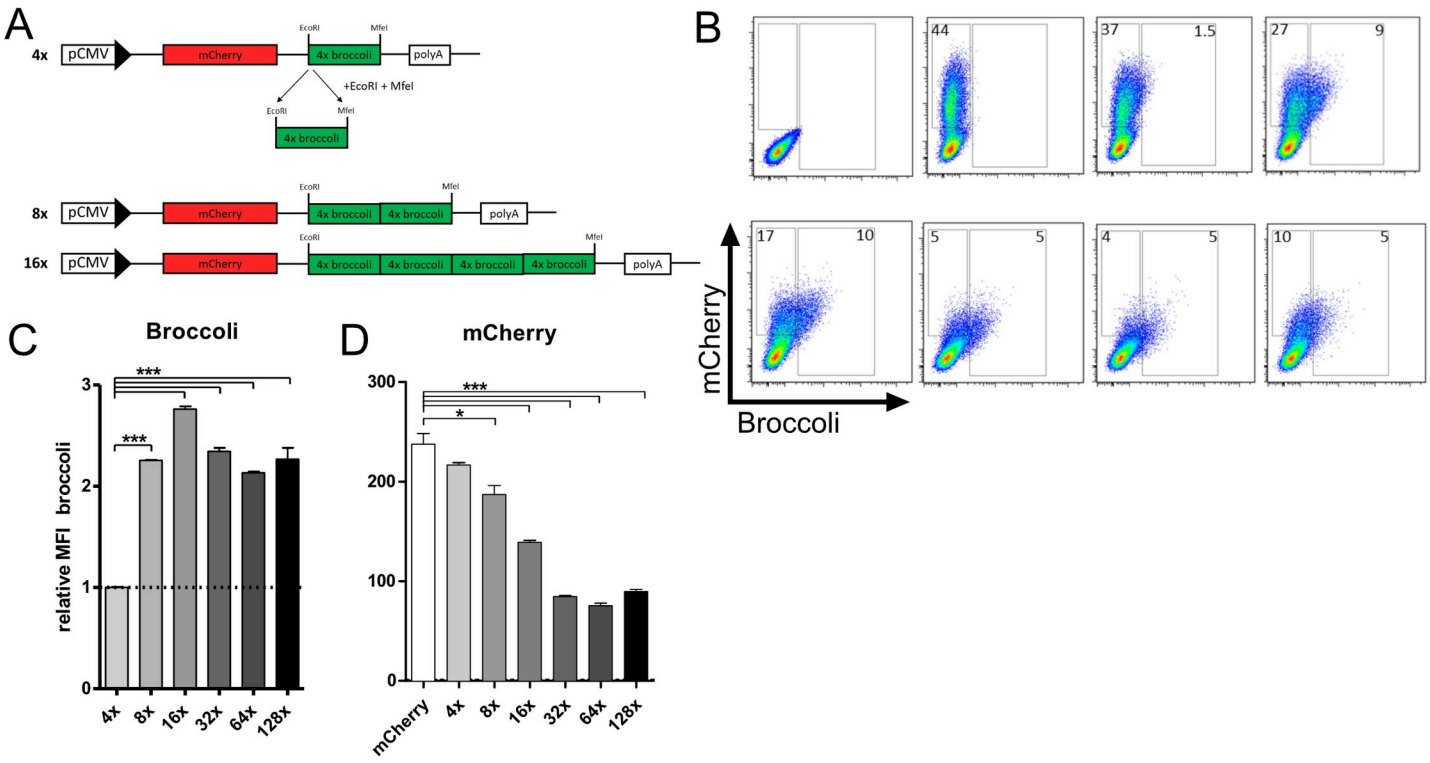

Fig 1. Broccoli tandem array synthesis and expression. (A) Cloning schematic of the constructs containing different copy numbers of Broccoli. (B, C, D) 293T cells were transfected with mCherry or 4x, 8x, 16x, 32x, 64x or 128x Broccoli and analyzed 24 hours post-transfection by flow cytometry. Percentage of Broccoli and mCherry positive cells shown in dot plots (B) and mean fluorescence intensity of Broccoli (C) and mCherry (D) compared between constructs. (D) The mean fluorescence intensity (MFI) of Broccoli in the graph was normalized to the 4x Broccoli construct and the MFI of the remaining constructs was calculated as follows: **(** (MFI **X**xBroccoli): (4xBroccoli) **)**. Data representative of three independent experiments. Statistical analysis performed by t-test (c, d). * $P<0.05$, ** $P<0.01$, *** $P<0.001$.

https://doi.org/10.1371/journal.pone.0244166.g001

This was to be expected and consistent with a decrease in transfection efficiency with increasing plasmid size (Figs 2A and S1). While only a modest decrease in mCherry expression strength was observed up to 8x Broccoli, mCherry expression dropped markedly with increasing numbers of Broccoli repeats (Fig 1D). Combined, these data indicate that increasing numbers of Broccoli repeats beyond 8x impairs gene expression of the reporter.

Flow cytometry data was further confirmed by fluorescence microscopy analysis. 293T cells were transfected with Broccoli-plasmids and 24 hours later incubated with DFHBI and analyzed by fluorescence microscopy. As observed by flow cytometry, both the number and intensity of mCherry-positive cells decreased with increasing copy number of the aptamer, and Broccoli intensity did not increase above 16x (Fig 2A). While 4x and 8x Broccoli displayed uniform cytoplasmic signal distribution, larger conctamers induced in the formation of green fluorescent aggregates (Fig 2B). For 128x Broccoli constructs, green fluorescence sometimes accumulated in the nucleus, indicative of impaired mRNA export. This was most prominent in NIH-3T3 cells (S4 Fig).

Broccoli analysis by microscopy represented an additional challenge, as fluorescence was very weak and bleaching occurred rapidly even when using highly sensitive electron-multiplying EMCCD cameras and low 488 nm laser excitation (S1 and S3 Videos) at higher frame rates. However, Broccoli, albeit exhibiting higher stability than its predecessors, still is a quite unstable aptamer [3]. As such it was possible to do time-lapse imaging of cells at low frame rate such that fluorescence could recover by fluorochrome exchange in a PAINT-like fashion [11] (S2 and S4 Videos) but without single-molecule sensitivity.

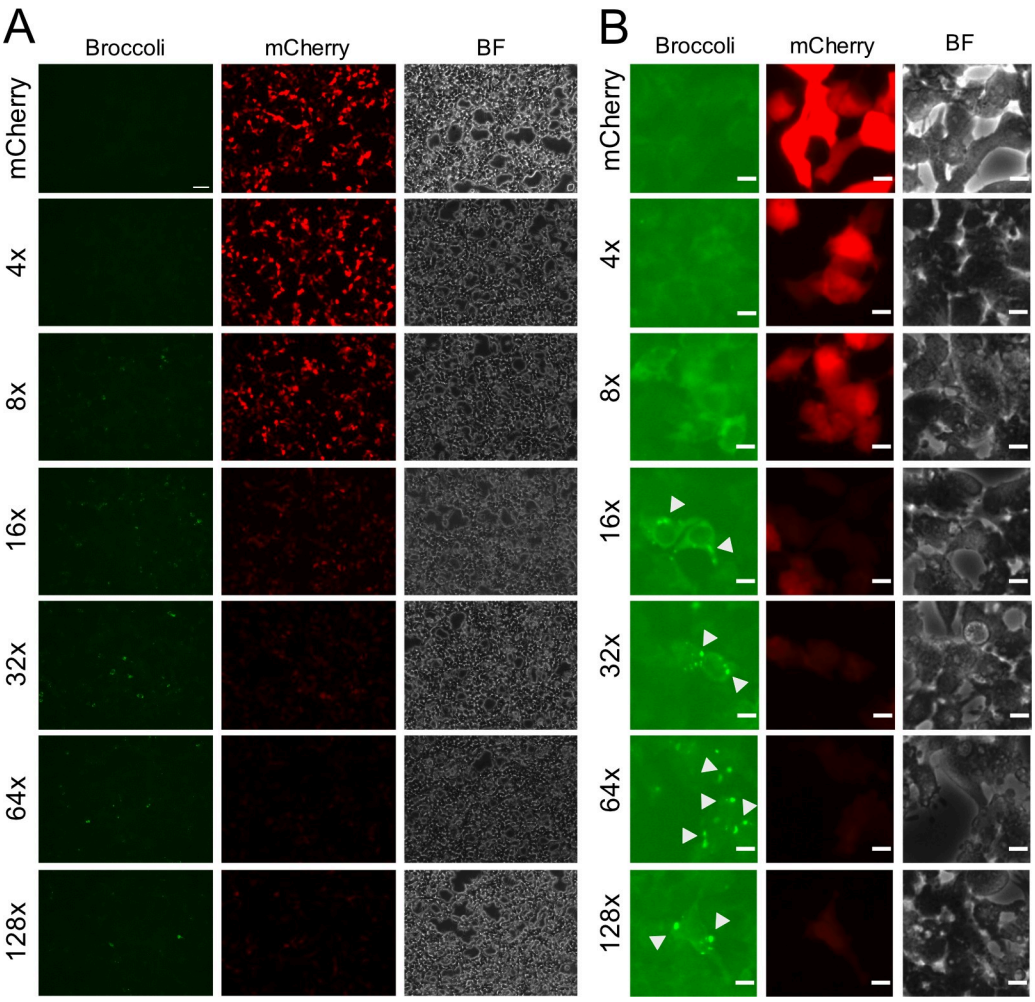

Fig 2. Broccoli exhibits punctate morphology. (A) 293T cells were transfected with mCherry, 4x, 8x, 16x, 32x, 64x, 128x Broccoli plasmids and analysed by microscopy for localization and morphology. (Scale bar = 75 μm) (B) Representative higher magnification inserts illustrating subcellular Broccoli distribution (Scale bars = 10 μm).

https://doi.org/10.1371/journal.pone.0244166.g002

Due to the highly structured and repetitive nature of the Broccoli concatemers, we hypothesized that 64x and 128x Broccoli would induce RNA aggregation. This might result in p-body or stress-granule formation, which are composed of arrested mRNAs or non-translating RNAs and their associated RNA-binding proteins [12,13]. The respective Broccoli constructs might thus provide a versatile tool to study these interesting cellular structures. To test this hypothesis, we transfected 293T cells with Broccoli plasmids and co-transfected with an additional, GFP-coding plasmid as a transfection indicator because Broccoli fluorescence was quenched by fixation. GFP-expression coincided very well with mCherry expression from the control plasmid a well as from the 4x Broccoli plasmid, indicating that most cells were transfected with both plasmids. We then stained for the p-body constituent DDX6 [14] or the stress-granule constituent eIF3a [15] and measured the DDX6 or eIF3a positive area (Fig 3A, 3B, 3E and 3F). As positive control, we used Sodium Arsenite [16] to induce both compartments (Fig 3C, 3D, 3G and 3H). We found that transfection with Broccoli plasmids did not induce the formation of p-bodies.

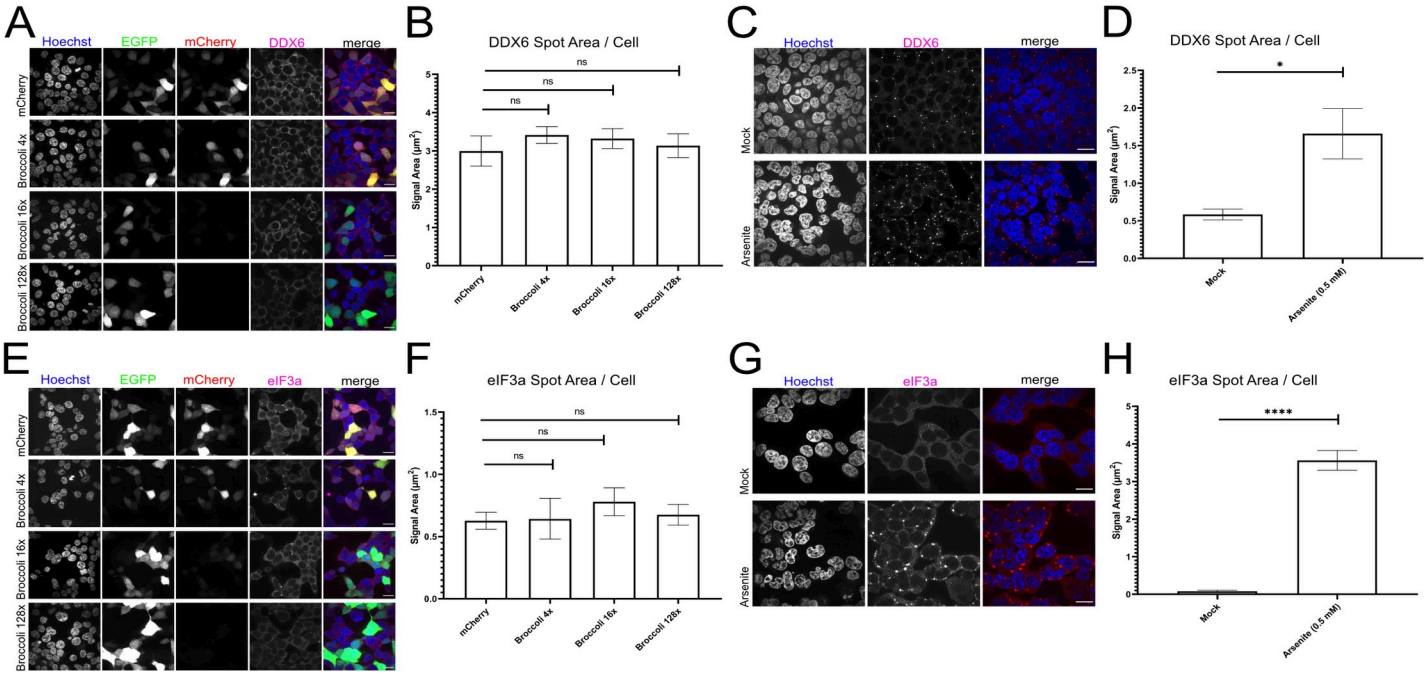

Fig 3. Broccoli concatamers do not induce p-bodies nor stress granules. (A) HEK293T cells were transfected with mCherry, 4x, 16x or 128x Broccoli as well as pEGFP-C1 as transfection control. After 24 hours, the cells were fixed and IF stained for DDX6. (B) The area of DDX6 positive spots in HEK293T cells from A was measured. No significant difference between the Broccoli versions was detectable. (3 Replicates; $N_{mCherry} = 3776$, $N_{4xBroccoli} = 3552$, $N_{16xBroccoli} = 3710$, $N_{128xBroccoli} = 5312$) (C) HEK293T cells were treated/mock-treated with 0.5 mM Sodium Arsenite for 1h to induce cell stress. Afterwards, the cells were fixed and stained for DDX6. (D) The area of DDX6-positive spots in HEK293T cells from (C) was measured. The difference between the mock treatment and the Arsenite treatment is statistically significant with $p = 0.0348$. (3 Replicates; $N_{Arsenite} = 9796$, $N_{Mock} = 12526$) (E) HEK293T cells were transfected and fixed for IF as described in A. The cells were afterwards IF stained for eIF3a. (F) The area of eIF3a positive spots in cells from E was measured. No significant difference between the Broccoli versions was detectable. (4 Replicates; $N_{mCherry} = 6030$, $N_{4xBroccoli} = 4674$, $N_{16xBroccoli} = 5860$, $N_{128xBroccoli} = 6992$) (G) HEK293T cells were treated with Sodium Arsenite as described in (C). After fixation the cells were IF stained for eIF3a. (H) The area of eIF3a positive spots in cells from G was measured. The difference between the mock treatment and the Arsenite treatment is statistically significant with $p < 0.0001$ (3 Replicates; $N_{Arsenite} = 10704$, $N_{Mock} = 8200$). All error bars show the standard error of the mean and all scale bars represent 20 μm.

https://doi.org/10.1371/journal.pone.0244166.g003

To check the integrity and quantify mRNAs expressed from our Broccoli reporters, we isolated total RNA from transfected 293T cells and performed Northern blots. Both mCherry and Broccoli sequences were independently probed for. In accordance with the immunofluorescence data shown in Figs 1 and 2A, both mCherry and Broccoli signals decreased with increasing copy numbers of Broccoli (Fig 4A and 4B, respectively). Both mCherry and Broccoli signals fell below the detection limit from 64x Broccoli onwards, indicative of impaired mRNA stability.

To directly confirm the effect of Broccoli concatemers on mRNA stability, we employed the RNA polymerase inhibitor Actinomycin D (Act-D) and performed pulse-chase experiments. 24h after transfection of 293T cells with mCherry only, 32x or 128x Broccoli plasmids, we applied Act-D for 2 and 6 h. Cells were harvested at the respective time points and qRT-PCR was performed for mCherry. The highly unstable c-myc mRNA were used as a control. As expected, c-myc detection levels progressively decreased from 2 to 6 h post Act-D treatment (Fig 4C). Interestingly, c-myc reduction was less pronounced in transfected cells regardless of the plasmid content, indicating that a transfection-induced stress response may interfere with cellular mRNA decay pathways. While mCherry mRNA levels dropped about 2-fold faster in presence of 32x Broccoli consistent with impaired mRNA stability, no further decrease in stability was observed for 128x Broccoli. In contrast to the highly unstable c-myc mRNA, the

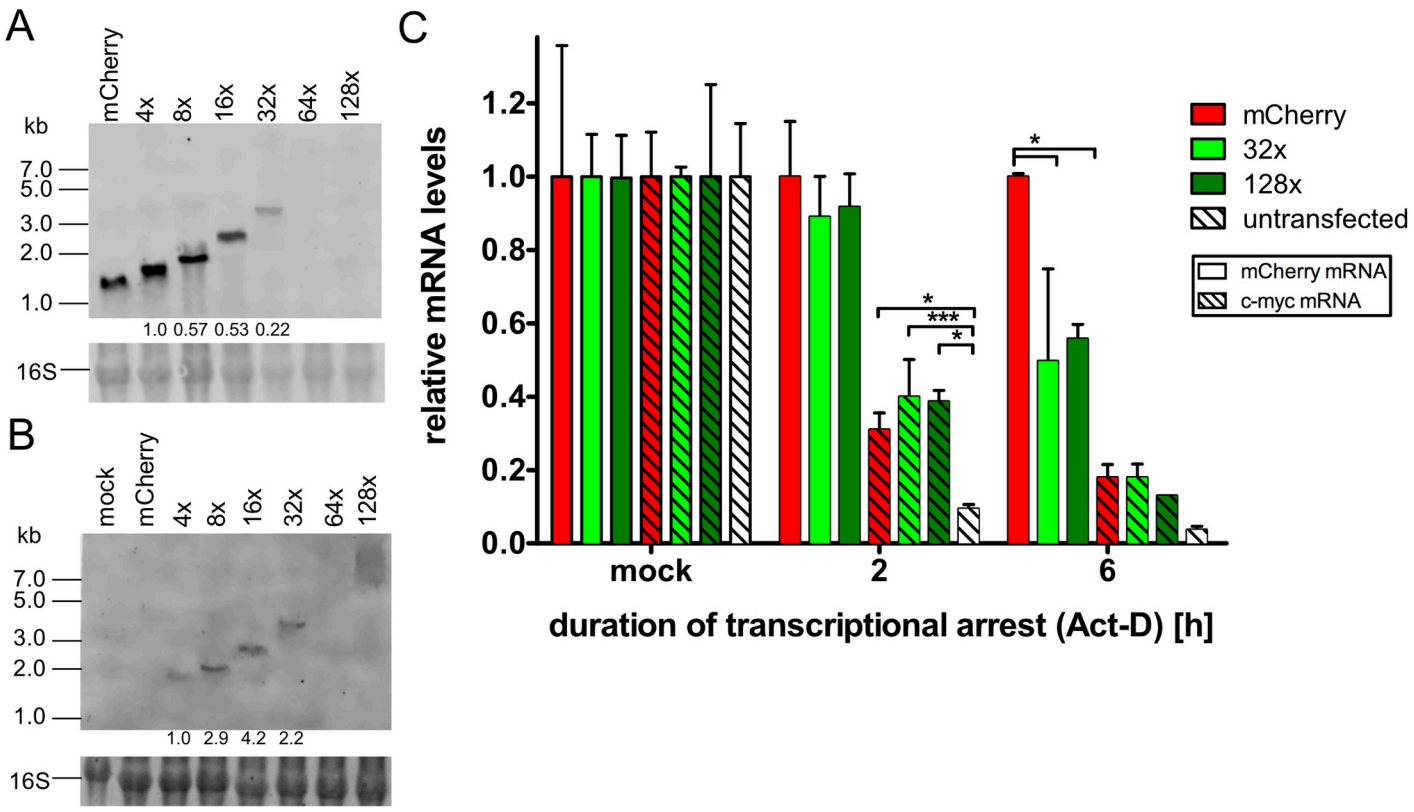

Fig 4. RNA of Broccoli is detectable up to 32 copies by Northern blot. 293T cells were transfected with mCherry or Broccoli plasmids and 10μg of isolated total RNA loaded on a denaturing gel for Northern blot. A fluorescently-labelled probe against mCherry (A) or Broccoli (B) was used to detect the respective RNAs. Intensities of mCherry and Broccoli RNA bands were measured using arbitrary values and normalized to either mCherry (A) or 4xBroccoli (B). 16s RNA was stained using ethidium bromide. (C) 293T cells were transfected with mCherry, 32x and 128x Broccoli plasmids. 24hours post-transfection, cells were collected (mock) or treated with actinomycin D for 2 or 6 hours. RNA was isolated at each time point and RT-qPCR performed for detection of mCherry and c-myc. Empty bars show mCherry transcription levels, striped bars represent c-myc transcription levels. Statistical analysis performed by 2-way ANOVA. * $P<0.05$, ** $P<0.01$, *** $P<0.001$.

https://doi.org/10.1371/journal.pone.0244166.g004

mRNA half-life of both the 32x and 128x Broccoli mRNA was in the range of about 6 h. While decreased mRNA stability thus accounts for the differences between the mCherry only and 32x Broccoli mRNA, it does not explain the additional loss in both mCherry and Broccoli Northern blot signal observed for the 64x and 128x reporters.

Broccoli is not detectable by fluorescence in stable cell lines

The study of transcription and protein expression from plasmids needs to consider features such as transient expression of genes; transfection efficiency between different plasmids; and variation in copy number of plasmids per cell. To circumvent these variables, we generated polyclonal 293T and HeLa cell lines that express either mCherry or 16xBroccoli. Cell lines expressing higher copy number of Broccoli were not possible to generate in our lab, as multiple attempts never resulted in full length Broccoli insertions but only recovered Broccoli fragments. No Broccoli fluorescence was detectable in the respective cell lines containing 16xBroccoli by FACS or fluorescence microscopy (Fig 5A). Nevertheless, the 16xBroccoli cells showed reduced fluorescence of mCherry compared to the mCherry only cells consistent with the Broccoli-induced impairment of mRNA stability. Accordingly, Northern blot analysis from total RNA isolated from the cell lines revealed lower levels of mCherry RNA in 16xBroccoli-cells (Fig 5B). In 16xBroccoli-HeLa cells, the RNA of mCherry did not reach detection levels.

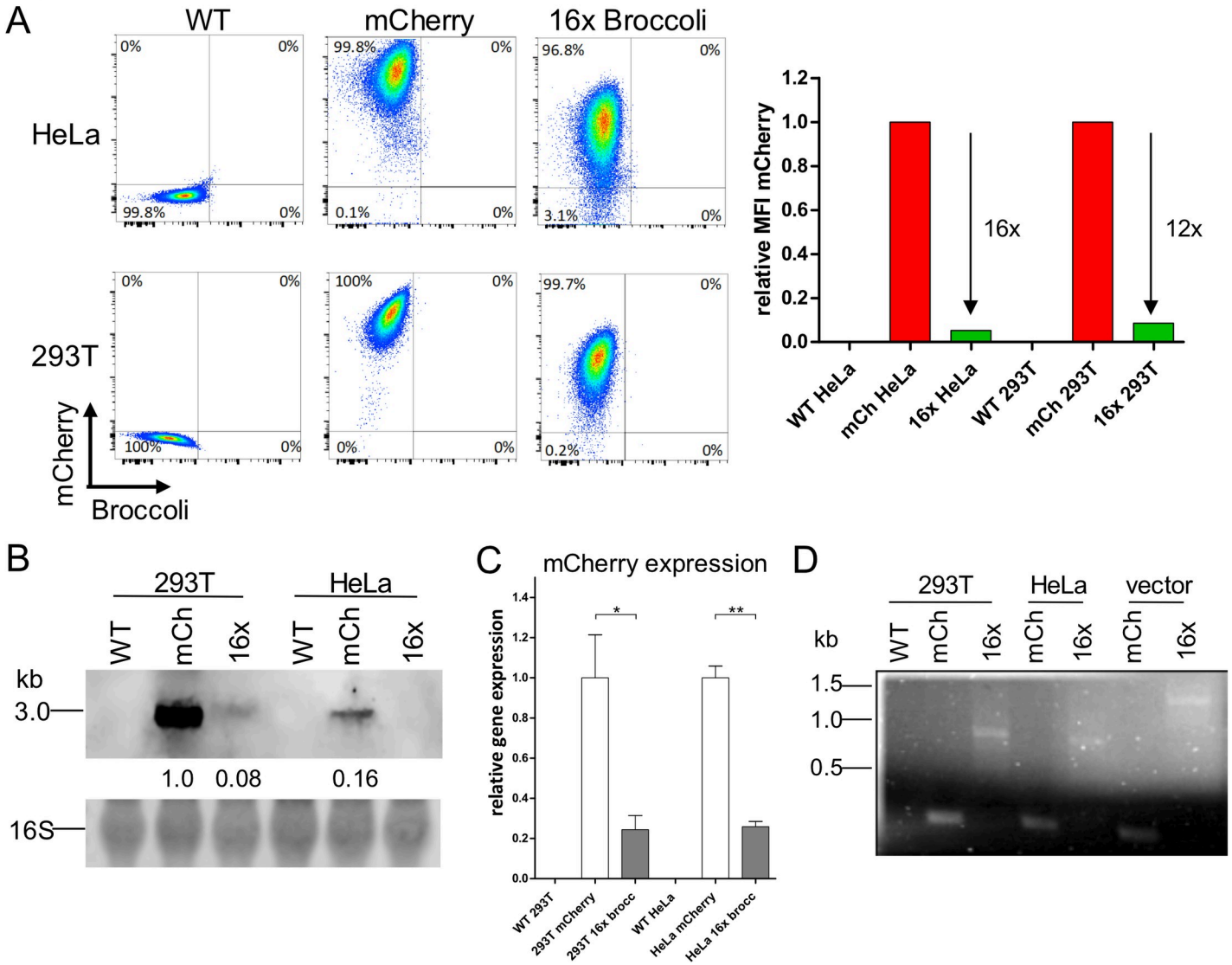

Fig 5. Polyclonal Broccoli-expressing cell lines showed reduced mCherry expression and no detectable Broccoli fluorescence. (A) Flow cytometry measurement of mCherry intensity in WT, mCherry or 16xBroccoli 293T or HeLa cells. (B) Northern Blot of mCherry RNA in the stable cell lines. RNA intensity was quantified and calculated relative to the 16S ribosomal band. All quantifications were further compared to the mCherry RNA in the mCherry-293T cells which was normalized to one. (C) RT-qPCR of mCherry. RNA was isolated from the stable cell lines, cDNA prepared and mCherry quantified by qPCR. Delta delta Ct of mCherry was calculated using GAPDH as the reference gene. Afterwards, all values were normalized to mCherry 293T cells. (D) Standard PCR for Broccoli from DNA isolated from 293T and HeLa cells expressing mCherry or 16x Broccoli (four lanes on the left side); lentiviral plasmid used for the generation of the mCherry and 16x Broccoli cell lines (two lanes on the right side). Contrast of gel image was optimized using the substract background function in Fiji (Fiji.sc). Statistical analysis performed by t-test (C). * $P<0.05$, ** $P<0.01$.

https://doi.org/10.1371/journal.pone.0244166.g005

Furthermore, mCherry detection by RT-qPCR revealed an approximate 80% drop in RNA levels in 16xBroccoli-cells (Fig 5C). To assess if we successfully integrated the full length of the 16 copies of Broccoli into our cells, we isolated genomic DNA and run a standard PCR using a forward primer at the 3'end of the mCherry sequence and a reverse primer at the 3'end of the final Broccoli repeat, covering the full length of Broccoli (where the expected length for 16xBroccoli would be 1278 bp). As a control, we performed PCR with the same primers on the lentiviral vector used to generate the cell lines. As expected, in the mCherry control vector and mCherry-cells we were unable to detect a Broccoli PCR product (Fig 5D). When the

16xBroccoli-vector was included as template we detected a band with the expected size of the full-length 16xBroccoli (Fig 5D). However, the band detected in both the 293T and HeLa cells expressing Broccoli were of smaller size, suggesting that the cells internally recombined some of the 16 copies of Broccoli sequence and generated a truncated sequence of Broccoli repeats. Despite continued effort, we were unable to sequence the integrated locus. Nevertheless, the length of the product indicated that at least 8x copies of Broccoli had been maintained (Fig 5D).

Broccoli is not sustained by the genome of mouse cytomegalovirus

RNA aptamers represent interesting tools to visualize viral gene expression. Cytomegalovirus genomes are easily manipulated using reverse genetics approaches [17]. The large genome of murine cytomegalovirus (MCMV) provides an interesting vector to insert long DNA sequences such as Broccoli to study viral gene expression at the single-cell level. In order to reduce the risk for homologous recombination and thus removal of the inserted Broccoli concatemers, we took advantage of a large deletion mutant that lacks the first 17 genes of MCMV (delm01-m17) but shows wild-type virus replication properties in fibroblasts *in vitro* [18]. We inserted either mCherry or its 16x and 32x Broccoli variants using traceless mutagenesis [17] driven by a CMV promoter. Correct insertion and integrity of the MCMV BAC containing 16x and 32x Broccoli was confirmed by restriction digests. We subsequently reconstituted the respective viruses expressing either mCherry only (MCMV-mCherry), 16xBroccoli (MCMV-16x) or 32xBroccoli (MCMV-32x). We infected NIH-3T3 cells directly from the reconstituted virus inoculum. At 6h p.i., we already observed an average of 80% infection rate in the samples infected with MCMV, which was evaluated by analyzing the percentage of mCherry-positive cells (Fig 6A). At 2, 4 and 6h p.i. a progressive increase in the mCherry mean fluorescence intensity (MFI) was evident (Fig 6B). As expected, cells infected with the MCMV-16x and MCMV-32x displayed lower mCherry levels than MCMV-mCherry only infected cells (Fig 6B). However, no Broccoli signal could be observed above background (Fig 6A and 6B). To check the integrity of the inserted Broccoli concatemers, we isolated DNA from cells infected with MCMV-mCherry, MCMV-16x and MCMV-32x, at 6 hours post-infection. We designed primers that bind at the 3'end of mCherry and at the 3'end of Broccoli in order to obtain the full length of the Broccoli concatemers by PCR (expected length for MCMV-16x is 1200 bp, and MCMV-32x is 2292 bp). For MCMV-16x, we detected one product of the correct size, however the PCR also yielded three more bands below 1000 bp indicative of genomic recombination (Fig 6C, middle lane). For the MCMV-32x sample, we did not observe a band matching the full length of Broccoli (Fig 6C, right lane). Instead, we detected three products at approximately 800, 600 and 400 bp. We conclude that concatemers of Broccoli are not sufficiently stable to be faithfully maintained within the MCMV genome even for a very limited number of passages.

Insertion of exonic sequences improves Broccoli fluorescence

Apparently, Broccoli concatemerization beyond 8 copies resulted in RNA aggregation and impaired both RNA localization and stability. In order to improve folding capacity of Broccoli, we created "spacers" between each 8 copies of Broccoli by insertion of partial sequences from exon 3 (151 nucleotides) or exon 5 (140 nucleotides), from the human GAPDH gene, at the 5' end of Broccoli (Fig 7A). Six new Broccoli expression plasmids were generated. We then transfected 293T cells and analyzed Broccoli and mCherry fluorescence by flow cytometry. While the percentage of transfected cells was similar between the exon-inserted and parental plasmids (Fig 7B), the insertions resulted in an increase in the MFI of Broccoli for both the exon5-

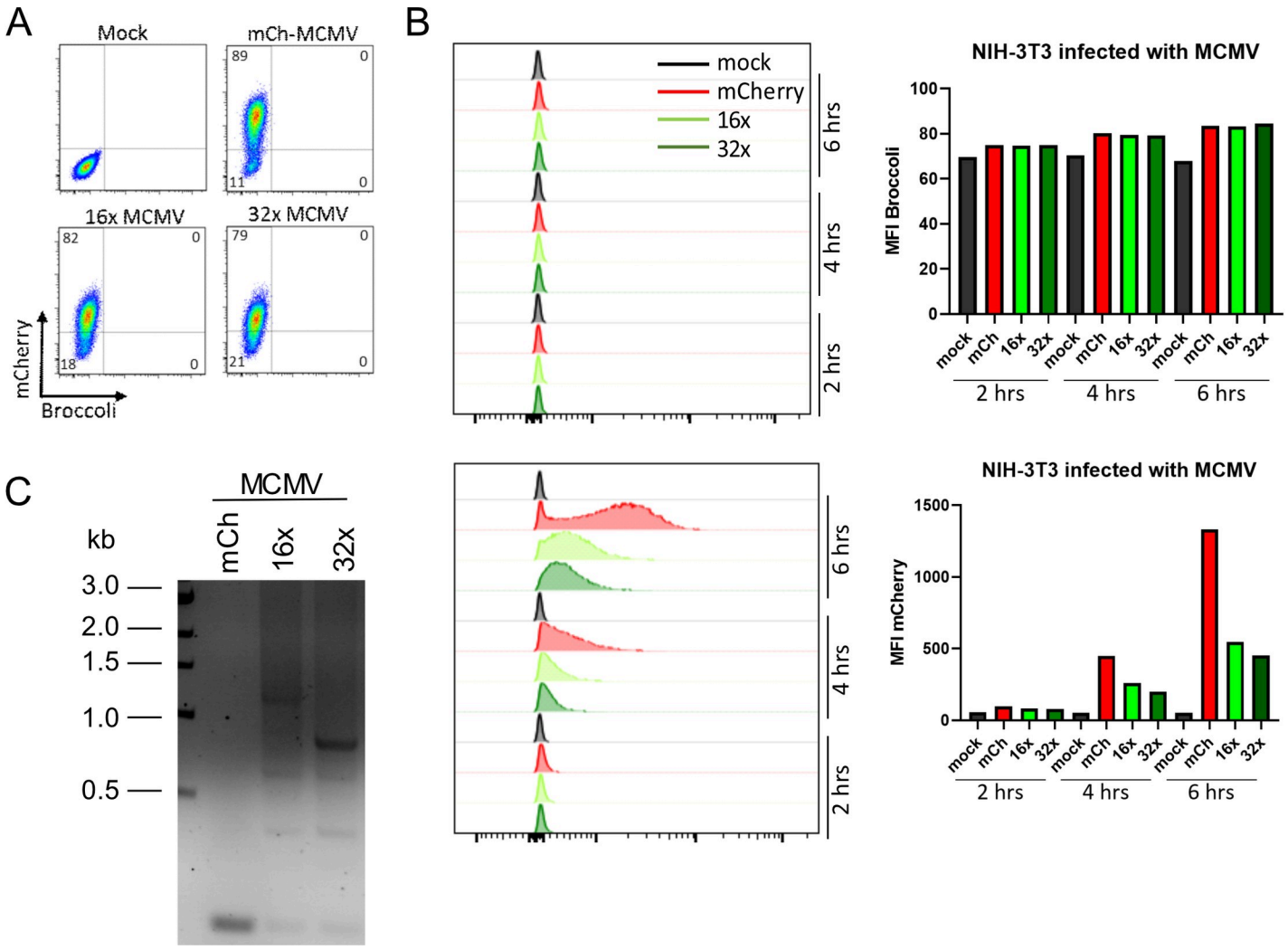

Fig 6. NIH-3T3 cells infected with Broccoli-MCMV viruses show reduced mCherry expression but no detectable Broccoli fluorescence. (A, B) NIH-3T3 cells were infected with undetermined MOI of mCherry-MCMV, 16x-MCMV or 32x-MCMV and analyzed by flow cytometry at 2, 4 or 6 hours post-infection. (A) Dot plots show cells at 6 hours post-infection. (B) Histograms and graph show progression of the viral infection/replication as shown by the mean fluorescence intensity of mCherry. (C) Standard PCR for Broccoli from DNA isolated from NIH-3T3 cells infected with mCh-MCMV, 16x-MCMV and 32x-MCMV, at 6 hours post-infection.

https://doi.org/10.1371/journal.pone.0244166.g006

and exon3-inserted plasmids (Fig 7C). Cells transfected with exon3-inserted plasmids showed significantly higher Broccoli MFI compared to exon5-inserted plasmids. Interestingly, the insertion of exons in between Broccoli repeats improved the MFI of mCherry, especially in cells transfected with 16xex3Broccoli compared to 16xBroccoli and in cells transfected with both 32xex3 and 32xex5 Broccoli compared to 32xBroccoli. We conclude that the incorporation of non-spliced, exon-derived spacers can improve both Broccoli and mCherry signals, which may be brought about through improved folding of broccoli concatemers resulting in increased stability of the transcript (see also S2 Fig).

Discussion

Fluorogenic RNA aptamers have the potential of surpassing the state-of-the-art real-time RNA imaging technology. They might induce less unexpected effects than fluorogenic proteins tagged to RNA, thereby delivering pictures of more physiological RNA transport and

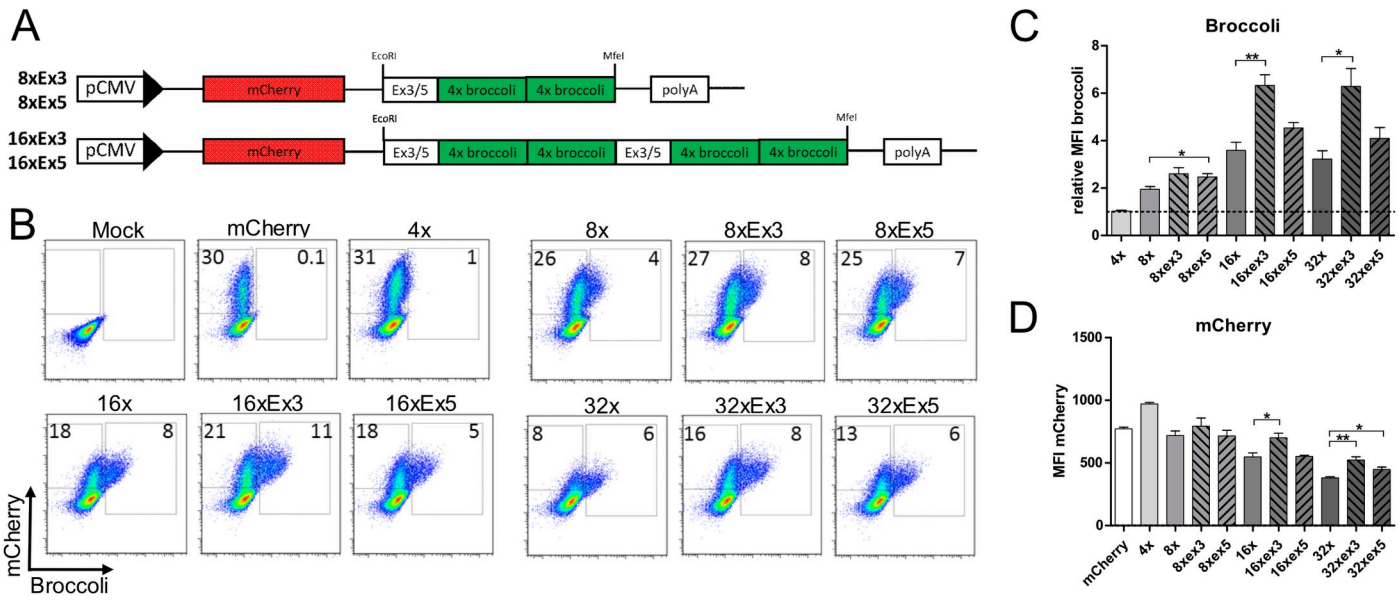

Fig 7. Expression profile of Broccoli tandem constructs with exonic inserts. (A) Cloning schematic of Broccoli with inserted exonic sequences, exon 3 or exon 5, from GAPDH gene of NIH-3T3 cells. (B, C, D) Flow cytometry data of 293T cells transfected with the different plasmids, collected and analysed 24 hours post-transfection. Comparison between the plasmids in regard to percentage of Broccoli and mCherry positive cells (B), mean fluorescence intensity of Broccoli (C) and mean fluorescence intensity of mCherry (D). (C) The values shown were normalized to the cells transfected with 4xBroccoli plasmid. Statistical analysis performed by t-test (C, D). * $P<0.05$, ** $P<0.01$.

https://doi.org/10.1371/journal.pone.0244166.g007

dynamics. Here, we report on the development of such an approach, tandem-Broccoli arrays, with the scope of utilizing the constructs in imaging mRNA transport and dynamics in herpes virus infection.

We found that fluorescence signals of Broccoli concatemers increased linearly up to eight Broccoli repeats within an mCherry-expressing mRNA. However, no further increase in signal could be achieved with larger concatemers, over 16 repeats. Moreover, further extension of the concatemers resulted in a loss of Broccoli signal, aggregation, reduced RNA stability and impaired mCherry expression. Interestingly, we observed the formation of aggregated green-fluorescent Broccoli "granules" in the cytoplasm but transfection of high-copy Broccoli concatemers did not trigger the formation of p-bodies or stress granules. In addition, we found nuclear accumulation of 128x Broccoli predominantly in NIH-3T3 cells. Considering the potential of Broccoli-RNAs to also form intermolecular interactions based on sequence complementarity, high-copy Broccoli concatemers may trigger liquid-liquid phase separation, not unlike of p-body formation [12]. Such RNA interaction-phase separation is a known mechanism that plays a role in disease developments [19]. However the fact that high copy number Broccoli concatamers formed aggregates which were undetectable in Northern blots, argues for a higly insoluble form that might not even be extractable by Trizol.

Aggregation of Broccoli-containing mRNAs might involve intermolecular interactions between multiple Broccoli-carrying RNAs, which are by default complementary to each other. Interestingly, the insertion of linker sequences between every eight Broccoli repeats improved both Broccoli and mCherry signals. The introduction of a sequence from GAPDH exon 3, predicted to exhibit low secondary structures, led to a strong boost of Broccoli signal, actually surpassing the theoretical doubling of fluorescence intensity. This illustrates that the availability of sufficient space for Broccoli folding may be an important prerequisite for obtaining high

signal Broccoli reporters. Nevertheless, we were still unable to increase fluorescence above the level provided by 16x Broccoli repeats.

Undesired Broccoli aggregation and plateauing of signal has not been reported by previous publications utilizing similar approaches though. In bacteria, Broccoli's predecessor Spinach continues increasing fluorescence, albeit only reaching ~17-fold enhancement by stringing 64 repeats together [9]. Here the inducibility, and not general overexpression, by a lac operon might reduce unwished behavior. The most successful approach so far in this context though was carried out by Li *et al.* utilizing a newly designed substrate, termed BI, that increases Broccoli folding and stability [10]. Future studies are directed to evaluate more advanced substrates in our experimental setting.

We also set out to establish cell lines which stably express Broccoli. However, we were unable to generate cells expressing high copy numbers of Broccoli using lentiviral vectors. The same was true when expressing Broccoli concatemers from the murine cytomegalovirus genome. Recombination occurred despite the MCMV genome being undersized due to the deletion of the first 17 MCMV genes. We conclude that the expression of Broccoli concatemers negatively impacts productive virus infection presumably due to the associated stress response, resulting in at least partial elimination of the Broccoli repeats within a few virus passages. However, we have to note that we were unable to successfully sequence the insertion sites despite numerous attempts which might be due to the repetitive nature of the construct.

Finally, we set out to find a way of utilizing the Broccoli aptamer in real-time imaging. This was complicated by the rapid bleaching of signal that occurs when exciting the fluorophore bound by RNA. However, the bleached signal recovered over time, presumably due to the dissociation of bleached substrate from the RNA scaffold and binding of new DFHBI or its derivatives. Using sufficiently long-time intervals between excitation should therefore enable long-term time-lapse imaging of RNA abundance.

Overall, we show here that RNA aptamer concatemers can be rapidly manipulated to enhance real-time RNA tracing, but strategies need to be developed and fine-tuned to overcome their impact on key aspects of RNA biology and avoid their rapid removal by homologous recombination.

Material and methods

Broccoli plasmids

We took advantage of the commercially available F30-2xdBroccoli construct (Geneart, Thermo Fisher) which is 234 nucleotides long. Short stem loop sequences to separate Broccoli aptamers from each other were added to this construct. The final F30-2xdBroccoli construct with the stem loops was flanked with EcoRI and MfeI sites, which were used to manifold the sequence to generate Broccoli concatemers. A single module, between EcoRI and MfeI, consists of 273 nucleotides and four DFHBI binding sites. This sequence was synthesized by Geneart (Thermo Fisher). We used a pCMV vector expressing mCherry downstream of a CMV promoter, and inserted Broccoli between the stop-codon of the mCherry protein and the SV40 poly-A-signal. To generate different-length Broccoli concatemers (S1 Table), the Broccoli sequence was extracted using EcoRI and MfeI and reinserted into the linearized vector, cut only with EcoRI, effectively doubling the sequence with each iteration (Fig 1).

To overcome folding restrictions caused by the length of the Broccoli constructs, we inserted exonic sequences from the GAPDH gene of NIH-3T3 cells, at the 5'end (EcoRI site) of 8 copies (8x) Broccoli. These exonic sequences (Ex3-Insert sequence: 5'-tcaccaggg ctgccatttgcagtggcaaagt ggagattgttgccatcaacgacccttcattgacctcaa ctacatggtctacatgttccagtatgactccactcacggcaaattcaacggcacagtcaa

ggccgagaatgggaagcttgt-3'; Ex5-Insert sequence: 5'-cccctctggaaagctgtggc gtgatggccgtgggg ctgcccagaacatcatccctgcatccactggtgctgccaaggct gtgggcaaggtcatcccagagctgaacgggaagctcactggcatggccttccgtgttccta -3') were PCR amplified, with primers containing EcoRI or MfeI sites (prW166 and prW167 or prW168 and prW169, S1 Table), from exon 3 (151 bp length) or exon 5 (140 bp ength) of the gene. The longer Broccoli concatemers containing exons were synthesized following the same cloning strategy described above (Fig 7).

Cell lines

NIH-3T3 cells were grown in Dulbecco's modified eagle medium (DMEM, Gibco) containing 10% newborn calf serum (NCS) and penicillin-streptomycin. HEK-293T and HeLa cells were grown in DMEM containing 10% fetal bovine serum (FBS) and penicillin-streptomycin.

Generation of the HeLa and HEK-293T cell lines expressing mCherry or mCherry-16x Broccoli

The pHRSIN.pSFFV MCS(+) pGK Hygro plasmid (referred from here onwards as pHRSIN) was kindly provided by Paul Lehner. MCherry or 16 copies (16x) of Broccoli was inserted into the multicloning site of the pHRSIN plasmid. The pHRSIN plasmid was digested with BamHI, followed by Klenow (New England Biolabs) treatment and afterwards KpnI and CIP. mCherry and 16xBroccoli plasmids were digested with AfeI and KpnI. Ligation of the correct sequences followed, using T4 ligase and incubation at room temperature. Afterwards, MAX Efficiency Stbl2 competent cells (Invitrogen) were transformed by heat-shock with the ligation reaction and grown in LB agar plates for clone selection. For confirmation, clones with the correct insertions were sequenced before proceeding. Due to the length of all constructs above 16xBroccoli, further cloning with the remaining Broccoli repeats into pHRSIN was not successful. HEK-293T or HeLa cells were transfected with pHRSIN, pHRSIN-mCherry, or pHRSIN-16xBroccoli plus psPAX2 and CMV.VSVg plasmids at a ratio 5:3:1, respectively. Following transfection, we collected the supernatant 48hrs later and transduced new HEK293T or HeLa cells. 48 hours later, cells were split and grown in media supplemented with 150μg/ml hygromycin for positive selection.

Broccoli expression and localization

HEK-293T cells were transfected with 4x, 8x, 16x, 32x, 64x or 128x Broccoli plasmids or a mCherry plasmid (control) in equimolar ratios, using the transfection reagent polyethylenimine (PEI, Polysciences). (Note: due to large differences in length between plasmids (see S1 Table for base pair number information), we co-transfected with a control plasmid, pEPkan-S (Adgene plasmid #41017) [20], which is not containing a sense-ORF for these cells, to equalize the DNA mass of each transfection sample). 24 hours later, the cell media was aspirated and PBS with 20μM GK132 DFHBI (more stable) or DFHBI-1T (less stable) was added and cells incubated at 37˚C for 30 minutes. Broccoli was either analyzed by flow cytometry (LSRII, BDbioscience) using DFHBI-1T or microscopy (GK132 DFHBI). HEK-293T and HeLa cell lines generated to express mCherry or 16x Broccoli were trypsinized, washed with PBS, incubated with PBS plus 20μM of DFHBI-1T for 30 minutes, and signals acquired by flow cytometry.

To assess transfection efficiency of the different Broccoli plasmids, HEK-293T cells were transfected with mCherry, 32x or 128x Broccoli together with 25ng of the plasmid pEGFP-C1 (adgene plasmid #6084–1). Cells were collected 24 hours post-transfection and analyzed by flow cytometry for mCherry versus GFP expression (no DFHBI was added).

Live-cell imaging

HEK-293T cells were co-transfected with Broccoli plasmids, labelled the next day with Hoechst 33342 (Thermofisher) and PFP-DFHBI for Broccoli and imaged using a Nikon spinning disc system consisting of a Yokogawa W2 and two Andor iXON888 cameras using NIS-Elements for image acquisition. A Nikon 100x 1.49 NA Apo-TIRF objective was used resulting in 130nm pixel size. The system was equipped with standard 405, 488, 561, 640 nm laser lines and corresponding filter sets. Since Broccoli-fluorescence was weak and sometimes barely distinguishable from cellular autofluorescence, Broccoli-expressing cells were identified in the 488-channel through their rapid bleach-behavior in live-camera mode. Upon identification, excitation was paused for 30 seconds until Broccoli fluorescence recovered and a single 4-channel Image (Hoechst, Broccoli, mCherry, SNAP) was taken using Nikon NIS AR 4.5 software.

Northern blot. HEK-293T cells were seeded on 10-cm dishes and transfected using PEI with 25μg of DNA at a ratio 1:3 DNA (mass): PEI (volume). 24 hours post-transfection, supernatant was aspirated and 2mL of TRI Reagent (Sigma Aldrich) were added per 10-cm dish to resuspend cells to a homogeneous lysate. RNA was purified as follows: 600μL of chloroform were added to each lysate, samples were vortexed vigorously and centrifuged; the aqueous phase was collected into a fresh tube where 1 volume of isopropanol was added and the samples were centrifuged; supernatants were removed and the precipitate washed two times with 75% ethanol and resuspended in 50μL nuclease-free water. To avoid DNA contamination, samples were submitted to DNase treatment using the Turbo DNA-free kit (Life Technologies) and the "rigorous DNase treatment" protocol according to the manufacturer's instructions. RNA was further purified by adding 1 volume of Roti-Aqua-P/C/I (Roth) followed by two 75% ethanol washes as described above. 10μg (for mCherry detection) or 20μg (for Broccoli detection) of RNA was resolved on a 1% agarose denaturing gel followed by blotting on a nylon membrane (Amersham Hybond-N^+, GE Healthcare). A probe for mCherry or for 4x Broccoli was synthesized by PCR using the 4x Broccoli plasmid as template and the primers prW150-prW151 for Broccoli and prW459-prW460 for mCherry. The probes were fluorescently labelled by including 10nM of Aminoallyl-dUTP-ATTO-680 (Jena Bioscience) in the PCR reaction. For hybridization, the membrane was incubated overnight at 60˚C together with the probes diluted in Church buffer (1% (w/v) BSA, 1mM EDTA, 0.5 M phosphate buffer, 7% (w/v) SDS). The probes were detected via the 700nm channel of the LI-COR Odyssey Imaging System.

Broccoli insertion into mouse cytomegalovirus. Insertion of Broccoli fragments into the BAC C3X delm01-m17 mutant (here onwards referred as pD2-BAC, previously described [18] and a kind gift from Zsolt Ruzsics), was performed using the FLPe-FRT system as follows. A transiently expressed pOri plasmid containing two Frt sites was linearized using ApaI. Afterwards, a NheI site was inserted by PCR-mutagenesis and amplification of the vector using primers prW442 (containing an ApaI site) and prW443 (containing a NheI site). The derived PCR product (pOri plasmid with ApaI and NheI sites) was used to ligate with mCherry or Broccoli fragments digested ApaI and NheI as well, resulting in the plasmids pOri-mCherry; pOri-16xBroccoli and pOri-32xBroccoli. Electro-competent E.Coli (GS1783), containing the pD2 BAC, were transfected with the different pOri plasmids together with a helper plasmid (pGPS-FLPe, a kind gift from Zsolt Ruzsics) which expresses the FLPe-recombinase. This led to the generation of different C3X BAC hereon referred to as MCMV-mCherry, MCMV-16x and MCMV-32x (S2 Table).

PCR for Broccoli

To detect insertion of Broccoli sequences in the originated plasmids; cell lines; or MCMV, midipreps were prepared for each plasmid, and DNA was isolated from the designated stable

cell line or from NIH-3T3 cells infected with MCMV. For plasmids 1-4ng were used for each PCR reaction, while for genomic DNA 50-100ng was used. The primer pair prW645-646 was used to detect Broccoli inserted in the lentivirus vector pHRSIN or in the stable cell lines, and the pair prW695-761 to detect Broccoli in MCMV. These primers flank the whole Broccoli sequence by annealing to the 3' end of the mCherry sequence and the 3' end of the last Broccoli repeat, respectively. The annealing temperatures used were: 61˚C for prW645-646 and 50˚C for prW695-761. Each PCR reaction mix included: Taq polymerase, 10x buffer, DMSO, 0.2mM of dATP, dTTP, dCTP, 0.05mM of dGTP (Roche) and 0.15mM of 7-deaza-dGTP (7-deaza-2′-deoxyguanosine 5′-triphosphate, NEB).

Actinomycin D treatment and qPCR

HEK-293T cells were transformed with mCherry, 32x Broccoli or 128x Broccoli plasmids as described above. 24 hours post-transfection, 10μg/mL of actinomycin D was added to the cells. Three technical replicates were performed for each condition and plasmid. Cells were collected at 24hours post-transfection without any treatment (mock) or 2- and 6-hours post-treatment with actinomycin D. RNA was isolated from these cells and submitted to DNase treatment, as described above. From total RNA, 300ng were used to synthesize cDNA with the All-in-One cDNA synthesis supermix (Biotool) and according to the manufacturer's instructions. Gene expression of mCherry was evaluated by a 2-step qPCR using 30ng of cDNA, the primers prW741 and prW742 and SYBR qPCR mastermix (Bimake). The primers prW83 and prW84 for GAPDH and prW819 and prW820 for c-myc were used as references/controls. SyBr green measurements were acquired using a Roche LightCycler 96 machine.

Measurement of p-Body and stress granule induction by concatemeric Broccoli. 5 hours before transfection 10^5 HEK293T cells were seeded in each well of a fibronectin (Sigma-Aldrich) coated Ibidi 8-well chamber slide (Ibidi). The cells were transfected with 100ng of the mCherry/Broccoli plasmid and 100ng of the pEGFP-C1 plasmid as transfection control, using PEI as the transfection reagent. Immunofluorescence stainings were performed by fixation of the cells in 4% paraformaldehyde (PFA, Science Services) in Dulbecco's Phosphate Buffered Saline (D-PBS, Sigma-Aldrich). The cells were permeabilized with 0.1% TritonX-100 in D-PBS and subsequently blocked with 10% FCS in D-PBS. Afterwards the samples were incubated with the primary antibody, either anti-DDX6 (NB200-191, Novus Biologicals) or anti-eIF3a (PA5-17212, Thermofisher) in D-PBS. Finally, the samples were incubated with the secondary antibody Alexa-647 goat anti-rabbit (Thermofisher) and nuclei were stained using Hoechst 33342 (Thermofisher). For the positive controls, cells were cultivated as described above. For the experiments, cells were seeded on fibronectin coated Ibidi dishes and treated/mock-treated with 0.5 mM Sodium Arsenite (Merck) in DMEM with 10% FCS for 1h. Afterwards the cells were fixed and IF stained as described above. Cells were imaged using a Nikon spinning disc system consisting of a Yokogawa W2 and one Andor iXON888 camera using NIS-Elements for image acquisition. A Nikon 100x 1.45 NA objective was used resulting in 130nm pixel size. The system was equipped with standard 405, 488, 561, 640 nm laser lines and corresponding filter sets. Images were taken using Nikon NIS AR 5.1 software. Two 5x5 tilings of a single plane in each sample were acquired. For quantification, the images were loaded in FIJI. Cells were counted by thresholding on the Hoechst channel and masked objects were automatically counted. The signals of the DDX6 and eIF3a channels were measured by first selecting the cytoplasmic area of the transfected cells by thresholding on the EGFP signal (transfection control). Then we applied a low strength Gaussian blur filter on the DDX6/eIF3a channel, followed by thresholding of the signal spots. The thresholded

objects were automatically counted and their size measured in the masked cytoplasmic area with FIJIs "analyze particles" tool. Statistical analysis was conducted in GraphPad Prism 9 (GraphPad Software).

Supporting information

S1 Fig. Expression profile of Broccoli tandem constructs in 293T cells. (A, B) 293T cells were co-transfected with a plasmid expressing eGFP plus mCherry, 32x, or 128xBroccoli plasmids. Percentage and intensity of eGFP and mCherry positive cells were detected by flow cytometry 24 hours later and are shown in the dot plots (A) and histograms (B), respectively. To accurately detect eGFP, DFHBI was not added to the cells. Three technical replicates are shown in the graphs. (C) The same protocol was applied and cells were collected 24 hours post-transfection for RNA isolation. RT-qPCR was performed to measure mCherry expression. The values shown were normalized to mCherry transfected cells. Statistical analysis performed by t-test. * $P<0.05$, ** $P<0.01$, *** $P<0.001$.
(TIF)

S2 Fig. Expression profile of Broccoli tandem constructs with exonic inserts. (A) 293T cells were transfected with mCherry, 8xEx3, 8xEx5, 16xEx3, 16xEx5, 32xEx3, 32xEx5, 64xEx3 Broccoli plasmids and analysed by fluorescent microscopy. (B, C) Northern blot from RNA isolated from 293T cells transfected with Broccoli plasmids containing exonic sequences. Northern membranes were probed for mCherry (B) or Broccoli (C). Values below the membranes and in the graphs indicate the intensity of the bands relative to the 16S ribosomal band for each sample and normalized to cells transfected with mCherry (B) or 4x Broccoli (C). Scale bar = 25μm.
(TIF)

S3 Fig. Expression of 128x Broccoli induces nuclear aggregations in NIH-3T3 fibroblasts. NIH-3T3 cells were transfected with 128x Broccoli and imaged by widefied microscopy 24 h later. Two representative examples are shown. Scale bar = 10 μm.
(TIF)

S4 Fig. Full images of blots and gels depicted in Figs 3–5.
(TIF)

S1 Table. List of primers used.
(PDF)

S2 Table. List of constructs used.
(PDF)

S1 Video. 293T cells were transfected with mCherry 32x Broccoli and analysed by live cell spinning disk microscopy with consecutive 100 ms per frame. Rapid bleaching can be observed.
(M4V)

S2 Video. 293T cells were transfected with mCherry 32x Broccoli and analysed by live cell spinning disk microscopy with 100 ms per frame every 5s. Apparent bleaching is mostly omitted likely due to dye exchange.
(M4V)

S3 Video. 293T cells were transfected with mCherry 32x Broccoli and analysed by live cell spinning disk microscopy with consecutive 100 ms per frame. Rapid bleaching can be

observed.
(M4V)

S4 Video. 293T cells were transfected with mCherry 32x Broccoli and analysed by live cell spinning disk microscopy with 100 ms per frame every 7s. Apparent bleaching omitted likely due to dye exchange.
(M4V)

Acknowledgments

We thank Rudolph Reimer, Roland Thuenauer and Carola Schneider (LCI Imaging Center at HPI Hamburg and CSSB AFLM) for their imaging support.

Author Contributions

Conceptualization: Thomas Hennig, Lars Dölken, Jens B. Bosse.

Data curation: Marco R. Rink, Marisa A. P. Baptista.

Formal analysis: Marco R. Rink, Marisa A. P. Baptista, Felix J. Flomm.

Funding acquisition: Lars Dölken, Jens B. Bosse.

Investigation: Marco R. Rink, Marisa A. P. Baptista, Felix J. Flomm, Adam W. Whisnant, Jens B. Bosse.

Methodology: Marco R. Rink, Marisa A. P. Baptista, Felix J. Flomm, Thomas Hennig, Natalia Wolf, Jürgen Seibel, Lars Dölken.

Project administration: Lars Dölken.

Resources: Natalia Wolf, Jürgen Seibel.

Supervision: Lars Dölken.

Validation: Marco R. Rink, Felix J. Flomm, Lars Dölken, Jens B. Bosse.

Visualization: Marco R. Rink, Marisa A. P. Baptista, Felix J. Flomm.

Writing – original draft: Marco R. Rink, Marisa A. P. Baptista, Lars Dölken, Jens B. Bosse.

Writing – review & editing: Marco R. Rink, Marisa A. P. Baptista, Felix J. Flomm, Lars Dölken, Jens B. Bosse.

References

1. Paige JS, Wu KY, Jaffrey SR. RNA Mimics of Green Fluorescent Protein. Science. 2011; 333: 642–646. https://doi.org/10.1126/science.1207339 PMID: 21798953
2. Autour A, Jeng SCY, Cawte AD, Abdolahzadeh A, Galli A, Panchapakesan SSS, et al. Fluorogenic RNA Mango aptamers for imaging small non-coding RNAs in mammalian cells. Nat Commun. 2018; 9: 656. https://doi.org/10.1038/s41467-018-02993-8 PMID: 29440634
3. Filonov GS, Moon JD, Svensen N, Jaffrey SR. Broccoli: Rapid Selection of an RNA Mimic of Green Fluorescent Protein by Fluorescence-Based Selection and Directed Evolution. J Am Chem Soc. 2014; 136: 16299–16308. https://doi.org/10.1021/ja508478x PMID: 25337688
4. Song W, Filonov GS, Kim H, Hirsch M, Li X, Moon JD, et al. Imaging RNA polymerase III transcription using a photostable RNA–fluorophore complex. Nat Chem Biol. 2017; 13: 1187–1194. https://doi.org/10.1038/nchembio.2477 PMID: 28945233
5. You M, Jaffrey SR. Structure and Mechanism of RNA Mimics of Green Fluorescent Protein. Annu Rev Biophys. 2015; 44: 187–206. https://doi.org/10.1146/annurev-biophys-060414-033954 PMID: 26098513

6. Bertrand E, Chartrand P, Schaefer M, Shenoy SM, Singer RH, Long RM. Localization of ASH1 mRNA Particles in Living Yeast. Mol Cell. 1998; 2: 437–445. https://doi.org/10.1016/s1097-2765(00)80143-4 PMID: 9809065

7. Park HY, Lim H, Yoon YJ, Follenzi A, Nwokafor C, Lopez-Jones M, et al. Visualization of Dynamics of Single Endogenous mRNA Labeled in Live Mouse. Science. 2014; 343: 422–424. https://doi.org/10.1126/science.1239200 PMID: 24458643

8. Braselmann E, Wierzba AJ, Polaski JT, Chromiński M, Holmes ZE, Hung S-T, et al. A multicolor riboswitch-based platform for imaging of RNA in live mammalian cells. Nat Chem Biol. 2018; 14: 964–971. https://doi.org/10.1038/s41589-018-0103-7 PMID: 30061719

9. Zhang J, Fei J, Leslie BJ, Han KY, Kuhlman TE, Ha T. Tandem Spinach Array for mRNA Imaging in Living Bacterial Cells. Sci Rep-uk. 2015; 5: 17295. https://doi.org/10.1038/srep17295 PMID: 26612428

10. Li X, Kim H, Litke JL, Wu J, Jaffrey SR. Fluorophore-Promoted RNA Folding and Photostability Enables Imaging of Single Broccoli-Tagged mRNAs in Live Mammalian Cells. Angewandte Chemie Int Ed. 2020; 59: 4511–4518. https://doi.org/10.1002/anie.201914576 PMID: 31850609

11. Sharonov A, Hochstrasser RM. Wide-field subdiffraction imaging by accumulated binding of diffusing probes. Proc National Acad Sci. 2006; 103: 18911–18916. https://doi.org/10.1073/pnas.0609643104 PMID: 17142314

12. Standart N, Weil D. P-Bodies: Cytosolic Droplets for Coordinated mRNA Storage. Trends Genet. 2018; 34: 612–626. https://doi.org/10.1016/j.tig.2018.05.005 PMID: 29908710

13. Protter DSW, Parker R. Principles and Properties of Stress Granules. Trends Cell Biol. 2016; 26: 668–679. https://doi.org/10.1016/j.tcb.2016.05.004 PMID: 27289443

14. Stefano BD, Luo E-C, Haggerty C, Aigner S, Charlton J, Brumbaugh J, et al. The RNA Helicase DDX6 Controls Cellular Plasticity by Modulating P-Body Homeostasis. Cell Stem Cell. 2019; 25: 622–638.e13. https://doi.org/10.1016/j.stem.2019.08.018 PMID: 31588046

15. Jain S, Wheeler JR, Walters RW, Agrawal A, Barsic A, Parker R. ATPase-Modulated Stress Granules Contain a Diverse Proteome and Substructure. Cell. 2016; 164: 487–498. https://doi.org/10.1016/j.cell.2015.12.038 PMID: 26777405

16. Stoecklin G, Kedersha N. Ten Years of Progress in GW/P Body Research. Adv Exp Med Biol. 2012; 768: 197–211. https://doi.org/10.1007/978-1-4614-5107-5_12

17. Tischer BK, Smith GA, Osterrieder N. In Vitro Mutagenesis Protocols, Third Edition. Methods Mol Biology. 2010; 634: 421–430. https://doi.org/10.1007/978-1-60761-652-8_30

18. Čičin-Šain L, Bubić I, Schnee M, Ruzsics Z, Mohr C, Jonjić S, et al. Targeted Deletion of Regions Rich in Immune-Evasive Genes from the Cytomegalovirus Genome as a Novel Vaccine Strategy▽. J Virol. 2007; 81: 13825–13834. https://doi.org/10.1128/JVI.01911-07 PMID: 17913824

19. Jain A, Vale RD. RNA phase transitions in repeat expansion disorders. Nature. 2017; 546: 243–247. https://doi.org/10.1038/nature22386 PMID: 28562589

20. Tischer K, Einem J von, Kaufer B, Osterrieder N. Two-step Red-mediated recombination for versatile high-efficiency markerless DNA manipulation in Escherichia coli. Biotechniques. 2006; 40: 191–197. https://doi.org/10.2144/000112096 PMID: 16526409